Electronic supplementary material

Ni_2P enhances the activity and durability of Pt anode catalyst in direct methanol fuel cells

Jinfa Chang[a]†, Ligang Feng[b]†, Changpeng Liu[a], Wei Xing[a*] and Xile Hu[b*]

† These two authors contributed equally to the work.

a. State Key Laboratory of Electroanalytical Chemistry, Laboratory of Advanced Power Sources, Changchun Institute of Applied Chemistry, Chinese Academy of Sciences, Changchun 130022, PR China; Fax: 86-431-85685653, E-mail: xingwei@ciac.jl.cn

b. Institute of Chemical Sciences and Engineering, Ecole Polytechnique Fédérale de Lausanne (EPFL), ISIC-LSCI, BCH 3305, Lausanne 1015, Switzerland.
Fax: (+) 49 21 693 9305, E-mail: xile.hu@epfl.ch. Homepage: http://lsci.epfl.ch

1 Experimental details

1.1 Materials.

Sodium hypophosphite monohydrate (≥ 99.0%, $NaH_2PO_2 \cdot H_2O$), nickel chloride hexahydrate (≥ 98.0%, $NiCl_2 \cdot 6H_2O$), hexachloroplatinic acid ($H_2PtCl_6 \cdot 6H_2O$) were purchased from Aldrich Chemical Co. (USA). Vulcan carbon powder XC-72 was purchased from Cabot Co. (USA). Nafion solution (5%) was purchased from Dupont Co. (USA). Sulfuric acid (≥ 95.0%) and ethanol (≥ 99.7%) were purchased from Beijing Chemical Co. (China). All the chemicals were of analytical grade and were used as received. High purity nitrogen (≥ 99.99%), oxygen (≥ 99.99%) and carbon monoxide (≥ 99.99%) were supplied by Changchun Juyang Co Ltd. Ultrapure water (resistivity： $\rho \geq 18\ M\Omega cm^{-1}$) was used to prepare the solutions.

1.2 Material characterization.

1.2.1 X-Ray Diffraction (XRD)

All X-Ray diffraction (XRD) measurements were performed with a PW1700 diffractometer (Philips Co.) using a Cu Kα (λ = 1.5405 Å) radiation source operating at 40 kV and 40 mA. Fine powder sample was grinded then put into a glass slide and pressed to make a flat surface on top of the glass slide.

1.2.2 Energy Dispersive Analysis of X-ray (EDX)

All Energy dispersive X-ray detector spectrum (EDX) measurements were performed with an XL30 ESEM FEG field emission scanning electron microscope.

1.2.3 Raman Spectra

All Raman spectra were collected on a J-Y T64000 Raman spectrometer with 514.5 nm wavelength incident laser light. To ensure homogeneity of the samples, three spectra were recorded from different spots on the sample. Raman spectra were then normalized for the intensity of the G -band.

1.2.4 X-Ray Photoelectron Spectroscopy (XPS)

All X-Ray photoelectron spectroscopy (XPS) measurements were carried out on a Kratos XSAM-800 spectrometer to determine the surface properties of the catalysts. Al X-ray source was operated at 250 W and the take-off angle of the sample to analyzer was 45°. Survey spectra were collected at a pass energy (PE) of 187.85 eV over a binding energy range from 0 eV to 1300 eV. High binding energy resolution multiplex data for the individual elements were collected at a PE of 29.55 eV. During all XPS experiments, the pressure inside the vacuum system was maintained at 1×10^{-9} Pa. Before analysis, all samples were dried under vacuum at 80 ℃ overnight.

2 Electrochemical Characterization.

All electrochemical measurements were performed with an EG & G PARSTAT 4000 potentiostat/galvanostat (Princeton Applied Research Co., USA). The cells used were conventional three-compartment electrochemical cells. The saturated calomel electrode (SCE, Hg/Hg_2Cl_2) were used as the reference electrodes. All of the potentials reported are relative to the SCE electrode. A Pt disk with the surface area of 0.0314 cm^2 was used as a counter electrode. A glassy carbon thin film electrode (diameter d = 4 mm) was used as a working electrode.

All Cyclic Voltammetry measurements were carried out in reference to SCE in 0.5 M H_2SO_4 solution purged with high-purity N_2.

2.1 Preparation of Working Electrode.

The catalyst ink was prepared by ultrasonically dispersing a mixture containing 5 mg of catalyst, 950 μL of ethanol and 50 μL of a 5 wt. % Nafion solution. Next, 5 μL of the catalyst ink was pipetted onto a pre-cleaned working electrode.

Before electrochemical measurements, adsorption/desorption of hydrogen on metal nanoparticles surface were evaluated in 0.5 M H_2SO_4. The electrode potential was scanned between -0.2 V and 1.0 V vs. SCE at 50 mVs^{-1} for surface cleaning. The cyclic voltammetry measurement was carried out until the steady

voltammogram was obtained (about 10 cycles).

2.2 Cyclic Voltammetry Measurements.

Electrochemical methanol oxidation was e performed in 0.5M H_2SO_4 contain 1 M CH_3OH. MilliQ water was used as the solvent. The electrodes were cleaned by polishing with 0. 05 μm alumina powder suspension (water) followed by ultrasonic cleaning in deionised water before use.

2.3 CO Stripping.

99.99% pure CO was purged to the cells filled with 0.5 M H_2SO_4 electrolyte for 30 min while the working electrode was held at 0.2 V vs. SCE. N_2 was then purged to the system for 30 min to remove non-adsorbed CO before the measurements were made. The CO stripping was performed in the potential range of -0.2 ~ 1.0 V at a scan rate of 50 mV s^{-1}. The electrochemical surface areas (ECSA) and the tolerance to CO poisoning were estimated by the CO stripping test, assuming that the Coulombic charge required for the oxidation of the CO monolayer was 420 μC cm^{-2}.

2.4 Chronoamperometry Measurements.

To estimate the stability of the catalysts, the chronoamperometric (CA) experiments were performed in still 0.5 M H_2SO_4 and 1 M CH_3OH solutions at 0.6 V.

2.5 Electrochemical Impedance Measurements.

The electrochemical impedance spectra (EIS) were recorded at the frequency range from 100 kHz to 10 mHz with 10 points per decade. The amplitude of the sinusoidal potential signal was 5 mV.

2.6 MEA Fabrication and Single-cell Performance Test.

Nafion 117 (DuPont) was used as the proton exchange membranes and the pre-treatment of the Nafion membrane was accomplished by successively treating the membrane in 5 wt. % H_2O_2 solution at 80 ℃, distilled water at 80 ℃, 8 wt.% H_2SO_4 solution at 80℃ and then in distilled water at 80 ℃ again, for 30 min in each step.

Membrane electrode assemblies (MEAs) with a 9 cm^2 active cell area were fabricated using a 'direct paint' technique to apply the catalyst layer. The 'catalyst inks' were prepared by dispersing the catalyst nanoparticles into appropriate amounts of Millipore® water and a 5% recast Nafion® solution. Anode and cathode 'catalyst inks' were directly painted onto carbon paper (TGPH060, 20 wt.% PTFE, Toray). For all MEAs in this study, the cathode consisted of unsupported platinum black nanoparticles (27 $m^2 g^{-1}$, Johnson Matthey) at a standard loading of 4 mg cm^{-2}. The anode consisted of carbon supported Pt catalysts. A single cell test fixture consisted of machined graphite flow fields with direct liquid feeds and gold plated copper plates to avoid corrosion (Fuel Cell Technologies Inc.). Hot-pressing was conducted at 140 ℃ and 10 atm for 90 s.

Five different anode catalysts were investigated in this study: (I) 20 wt. % Pt on Vulcan XC-72 (Pt/C-H), (II) 20 wt. % Pt-P on Vulcan XC-72 (Pt-P/C), (III) 20 wt. % Pt-Ni on Vulcan XC-72 (Pt-Ni/C), (IV) 20 wt. % Pt on Ni_2P@Vulcan XC-72 (Pt-Ni_2P/C-30%), (V) 20 wt. % commercial Pt/C (Pt/C-JM). The anode catalyst loading of the Pt/C was 5 mg cm^{-2} including the mass of the carbon supports.

The MEA was fitted between two graphite plates in a punctual flow bed. The polarization curves were obtained using a Fuel Cell Test System (Arbin Instrument Corp.) under the operation conditions of 60 ℃. High purity O_2 (99.99 %) is applied as the oxidant at 200 ml /min as the cathode atmosphere and 1 M methanol as the reactant feed at the anode side at 20 ml/min. The potential range is from the open circuit potential to 0.1V, and one point is collected every 0.05V where a delay of 1 minute was applied to get the steady state plots. Both sides are under ambient pressure.

3 Supporting Table and Figures

Table S1. Particle size comparison for various Pt-based catalysts used in this work.

Samples	Pt-Ni_2P/C-10%	Pt-Ni_2P/C-20%	Pt-Ni_2P/C-30%	Pt-Ni_2P/C-40%	Pt-Ni_2P/C-50%	Pt/C-JM
Particles size[a] (nm)	2.60	2.48	2.39	2.60	2.57	3.02
Particles size[b] (nm)	2.85	2.68	2.52	2.78	2.65	3.25

[a] Obtained from the measurement of TEM.

[b] Calculated from Scherrer equation[1]: $L = \frac{0.9\lambda_{K\alpha 1}}{B_{(2\theta)}\cos\theta_{max}}$

Where L is the average particle size, $\lambda_{K\alpha 1}$ is 1.54056 Å, and $B_{(2\theta)}$ is in radians.

Table S2 Electrochemical surface area (ECSA) estimated from hydrogen absorption and CO stripping experiments and the peak potentials for CO stripping.

Sample	ECSA[a] ($m^2\ g^{-1}$)	ECSA[b] ($m^2\ g^{-1}$)	Peak Potential (V vs. SCE)
Pt-Ni_2P/C-10%	55.74	51.46	0.614
Pt-Ni_2P/C-20%	60.15	60.18	0.607
Pt-Ni_2P/C-30%	69.34	70.57	0.591
Pt-Ni_2P/C-40%	59.73	63.30	0.606
Pt-Ni_2P/C-50%	37.04	44.34	0.610
PtNi/C	50.53	48.66	0.605
PtP/C	56.10	51.54	0.607
Pt/C-JM	54.91	57.34	0.623
Pt/C-H	39.67	40.50	0.666

[a] The ECSA of the catalysts integration from the hydrogen absorption.

b The ECSA of the catalysts integration from the CO stripping experiment.

Table S3 Mass activity and specific activity expressed as the positive scan peak current for all Pt/C catalysts in 1 M CH_3OH and 0.5 M H_2SO_4.

Sample	Mass Activity (A g^{-1}_{Pt})	Specific Activity (A m^{-2})
Pt-Ni_2P/C-10%	724.72	24.30
Pt-Ni_2P/C-20%	857.19	28.11
Pt-Ni_2P/C-30%	1431.68	40.49
Pt-Ni_2P/C-40%	1039.53	32.84
Pt-Ni_2P/C-50%	590.47	26.60
PtNi/C	492.51	18.41
PtP/C	419.60	16.20
Pt/C-JM	270.46	9.36
Pt/C-H	192.97	6.59

Table S4 The positive scan peak current density normalized as specific activity and mass activity for the Pt-Ni_2P/C-30% catalyst and other recently reported catalysts.

Catalysts	Specific Activity (mA cm^{-2})	Mass Activity (A g^{-1}_{Pt})	Scanning rate (mV/s)	Condition	References
Pt-Ni_2P/C-30%	4.05	1432	50	0.5 M H_2SO_4 + 1 M CH_3OH	This work
Pt_3Au/N-G		417	50	0.5 M H_2SO_4 + 0.5 CH_3OH	2
Pt/N-G		354	50	0.5 M H_2SO_4 + 1 M CH_3OH	3
Pt/TiO_2@N-C		500	50	0.5 M H_2SO_4 + 1 M CH_3OH	4
$Pd_{53}Pt_{47}$-FNMs		350	50	0.5 M H_2SO_4 + 1 M CH_3OH	5
Pt–WC/graphene		687	50	1 M H_2SO_4 + 1 M CH_3OH	6
Pt_3Zn/C	0.95	270	50	0.1 M H_2SO_4 + 0.5 CH_3OH	7
Pt-Ni-P	3.85		50	0.5 M H_2SO_4 + 0.5 CH_3OH	8
Ni@Pt nanotubes	1.5		50	0.5 M H_2SO_4 + 0.5 CH_3OH	9
$Pt_{3.6}Au_1$	0.6		50	0.5 M H_2SO_4 + 1 M CH_3OH	10
Pt/C_{40}-CeO_2	9		50	0.5 M H_2SO_4 + 0.5 CH_3OH	11

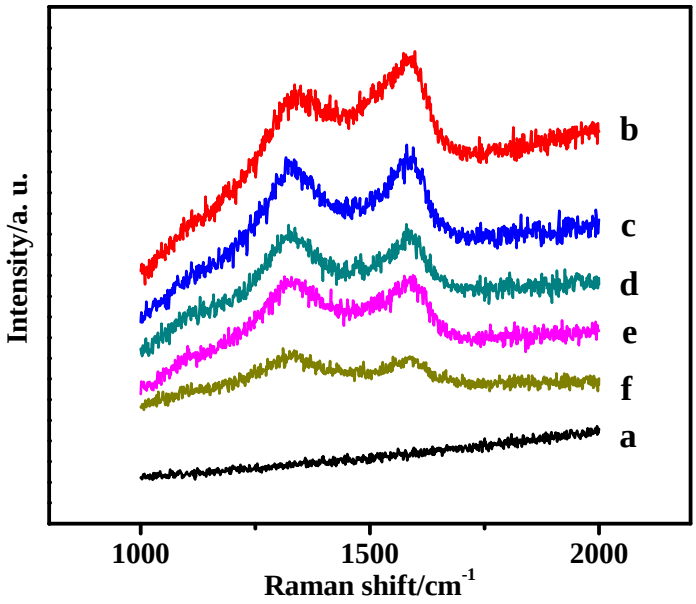

Figure S1. Raman spectra of Ni_2P (a), Ni_2P/C-10% (b), Ni_2P/C-20% (c), Ni_2P/C-30% (d), Ni_2P/C-40% (e) and Ni_2P/C-50% (f).

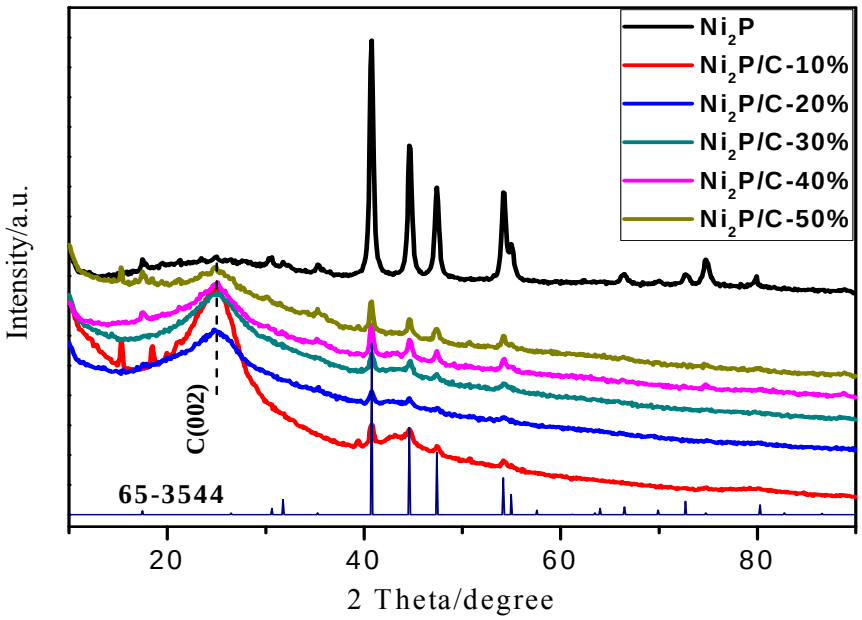

Figure S2. XRD patterns of Ni_2P and Ni_2P/C samples. x% denotes the loading of Ni_2P on C.

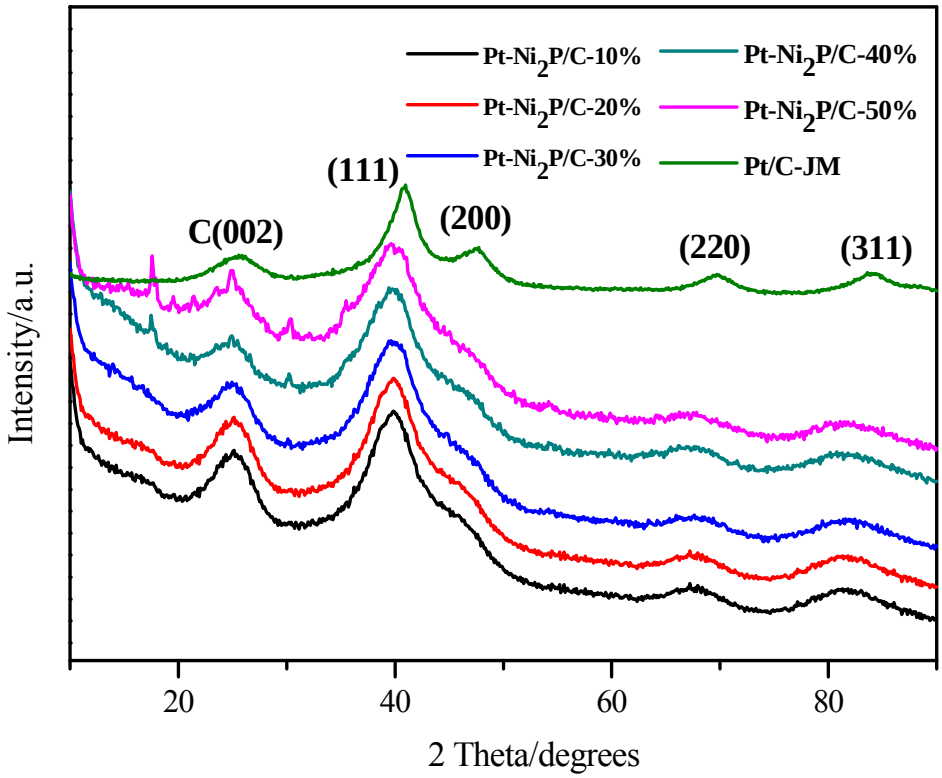

Figure S3. XRD patterns of Pt-Ni_2P/C and commercial Pt/C catalysts. The diffraction peaks come from Pt.

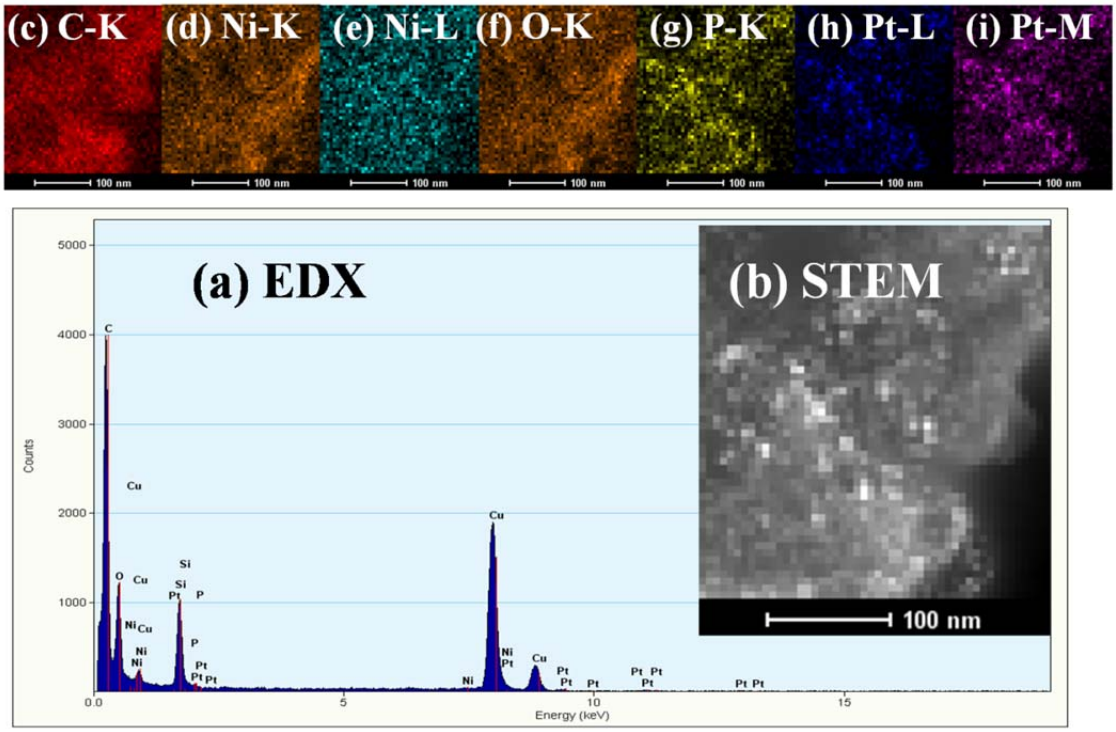

Figure S4. (a) EDX, (b) STEM, (C-I) Elemental mapping images of the Pt-Ni_2P/C-30% catalyst.

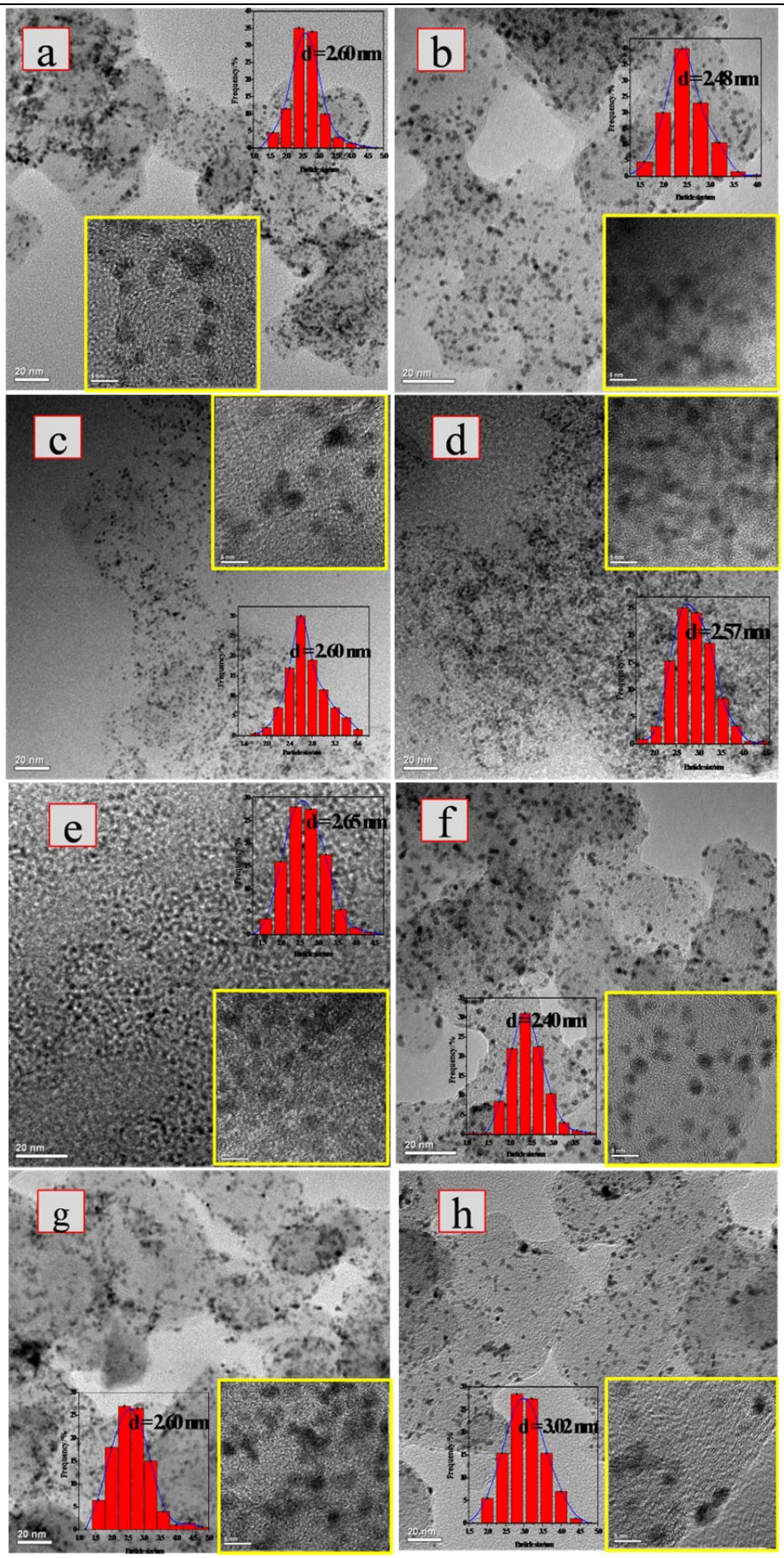

Figure S5. TEM for (a) Pt-Ni_2P/C-10%, (b) Pt-Ni_2P/C-20%, (c) Pt-Ni_2P/C-40%, (d) Pt-Ni_2P/C-50%, (e)

Pt-Ni/C, (f) Pt-P/C, (g) Pt/C-H, and (h) Pt/C-JM catalysts. Insets are the corresponding particle size distribution histograms and HR-TEM images.

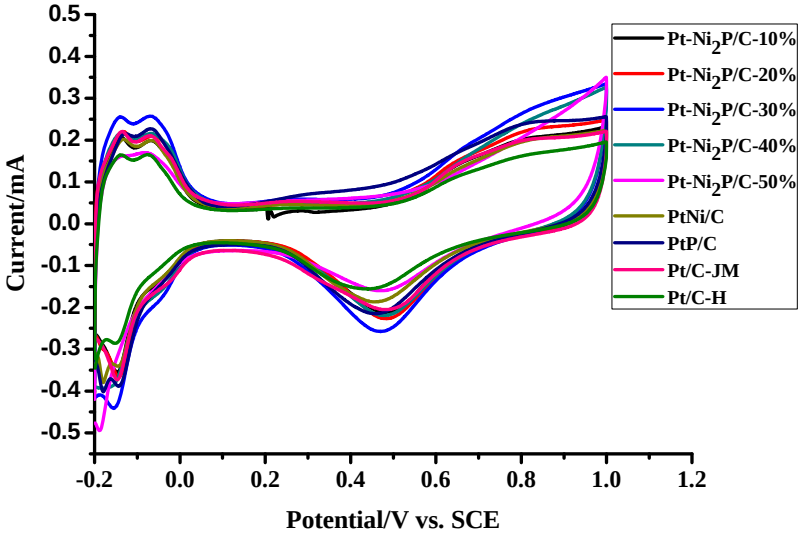

Figure S6. Typical cyclic voltammograms of Pt-Ni_2P/C-10 %, Pt-Ni_2P/C-20 %, Pt-Ni_2P/C-30 %, Pt-Ni_2P/C-40 %, Pt-Ni_2P/C-50%, Pt-Ni/C, Pt-P/C, Pt/C-JM and Pt/C-H catalysts in 0.5 M H_2SO_4.

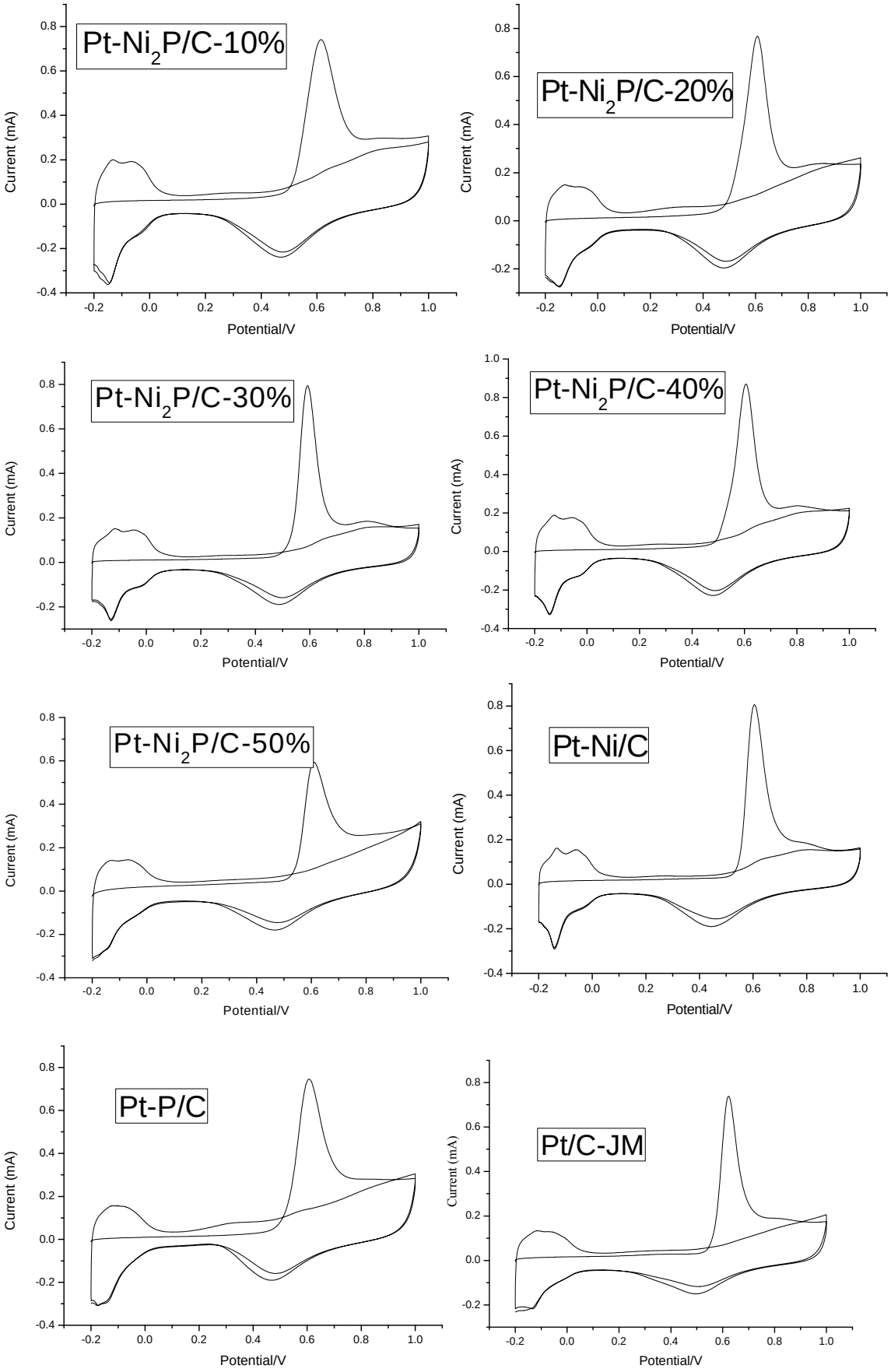
Pt-Ni2P/C-10%
Pt-Ni2P/C-20%
Pt-Ni2P/C-30%
Pt-Ni2P/C-40%
Pt-Ni2P/C-50%
Pt-Ni/C
Pt-P/C
Pt/C-JM
Current (mA)
Potential/V

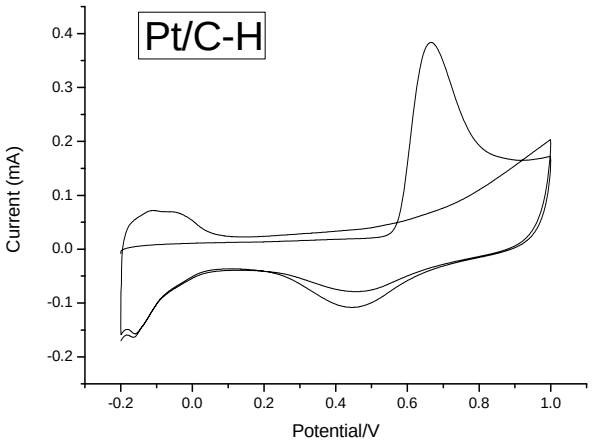

Figure S7. Illustration of the CO tolerance of various Pt-based catalysts used in this study by stripping voltammetry of adsorbed CO. Exposure of the electrode to a CO saturated solution at 0.20 V for 30 min was followed by purging the solution with N_2 for 20 min and a CV scan. Scanning rate was 50 mV s^{-1} and 0.5 M H_2SO_4 was used as the supporting electrolyte.

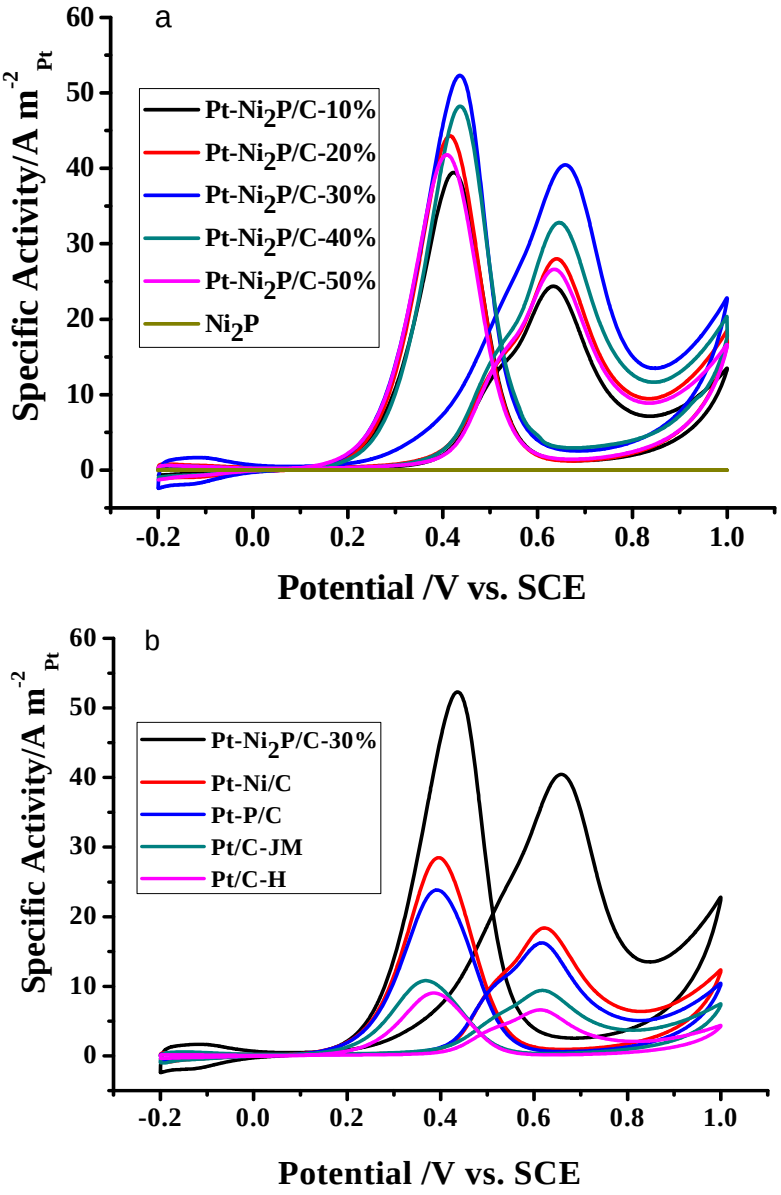

Figure S8. The specific activity of various Pt-based catalysts employed in this work illustrated by the cyclic voltammograms in 0.5 M H_2SO_4 solution containing 1 M CH_3OH at a scan rate of 50 mV s^{-1}.

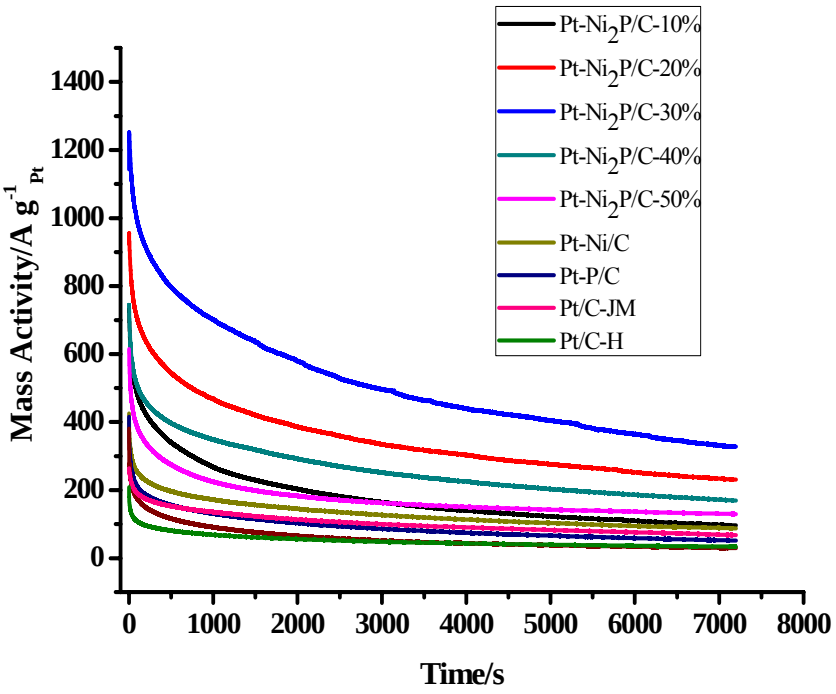

Figure S9. Chronoamperometric curves of different catalysts in 0.5 M H_2SO_4 solution containing 1 M CH_3OH at 0.6 V.

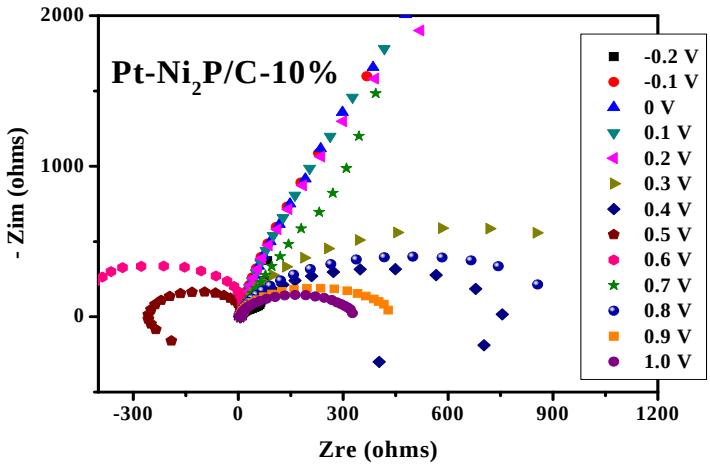
Pt-Ni2P/C-10%
- Zim (ohms)
Zre (ohms)
-0.2 V
-0.1 V
0 V
0.1 V
0.2 V
0.3 V
0.4 V
0.5 V
0.6 V
0.7 V
0.8 V
0.9 V
1.0 V

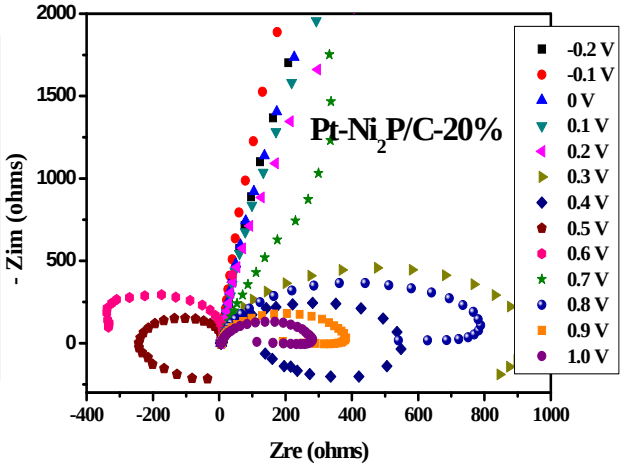
Pt-Ni2P/C-20%
- Zim (ohms)
Zre (ohms)
-0.2 V
-0.1 V
0 V
0.1 V
0.2 V
0.3 V
0.4 V
0.5 V
0.6 V
0.7 V
0.8 V
0.9 V
1.0 V

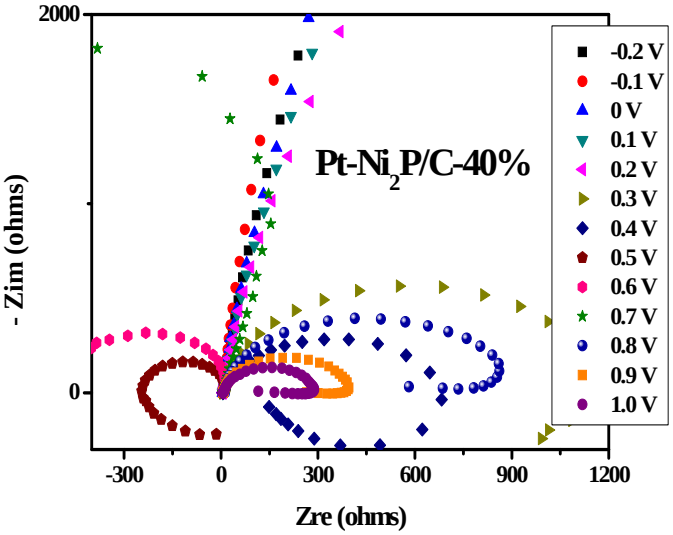
Pt-Ni2P/C-40%
- Zim (ohms)
Zre (ohms)
-0.2 V
-0.1 V
0 V
0.1 V
0.2 V
0.3 V
0.4 V
0.5 V
0.6 V
0.7 V
0.8 V
0.9 V
1.0 V

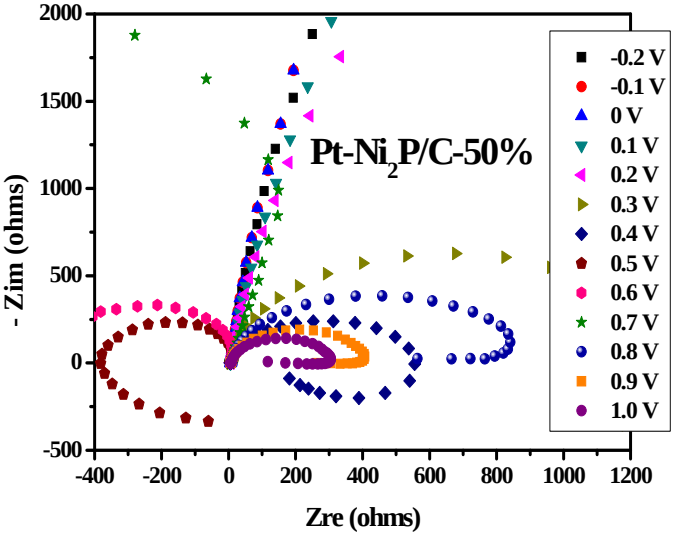
Pt-Ni2P/C-50%
- Zim (ohms)
Zre (ohms)
-0.2 V
-0.1 V
0 V
0.1 V
0.2 V
0.3 V
0.4 V
0.5 V
0.6 V
0.7 V
0.8 V
0.9 V
1.0 V

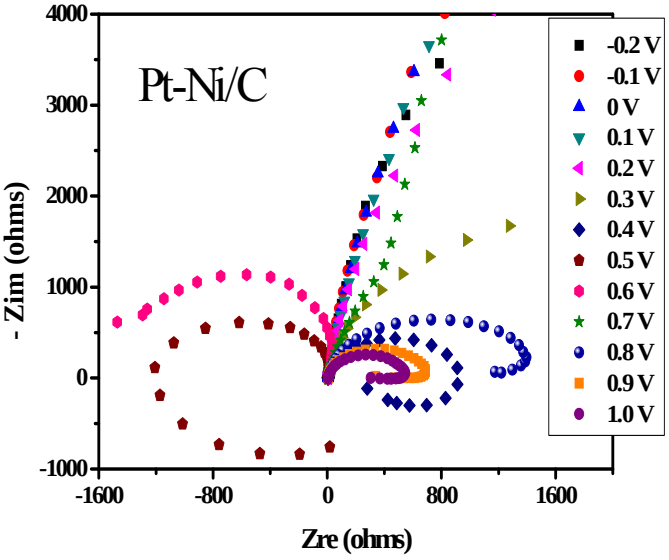
Pt-Ni/C
- Zim (ohms)
Zre (ohms)
-0.2 V
-0.1 V
0 V
0.1 V
0.2 V
0.3 V
0.4 V
0.5 V
0.6 V
0.7 V
0.8 V
0.9 V
1.0 V

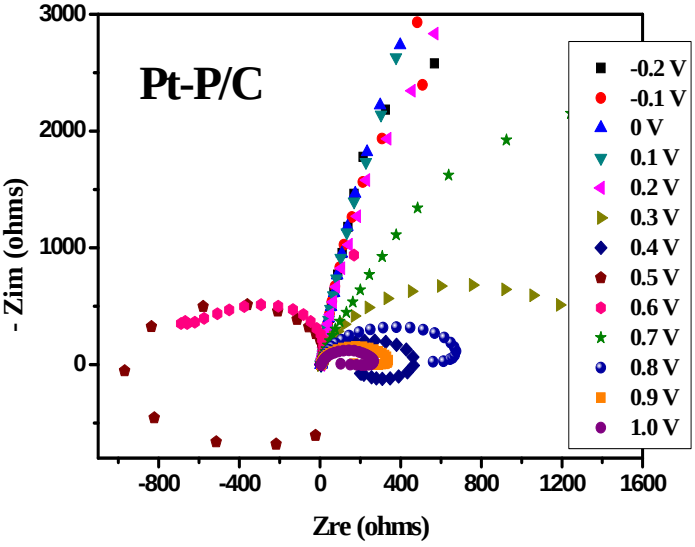
Pt-P/C
- Zim (ohms)
Zre (ohms)
-0.2 V
-0.1 V
0 V
0.1 V
0.2 V
0.3 V
0.4 V
0.5 V
0.6 V
0.7 V
0.8 V
0.9 V
1.0 V

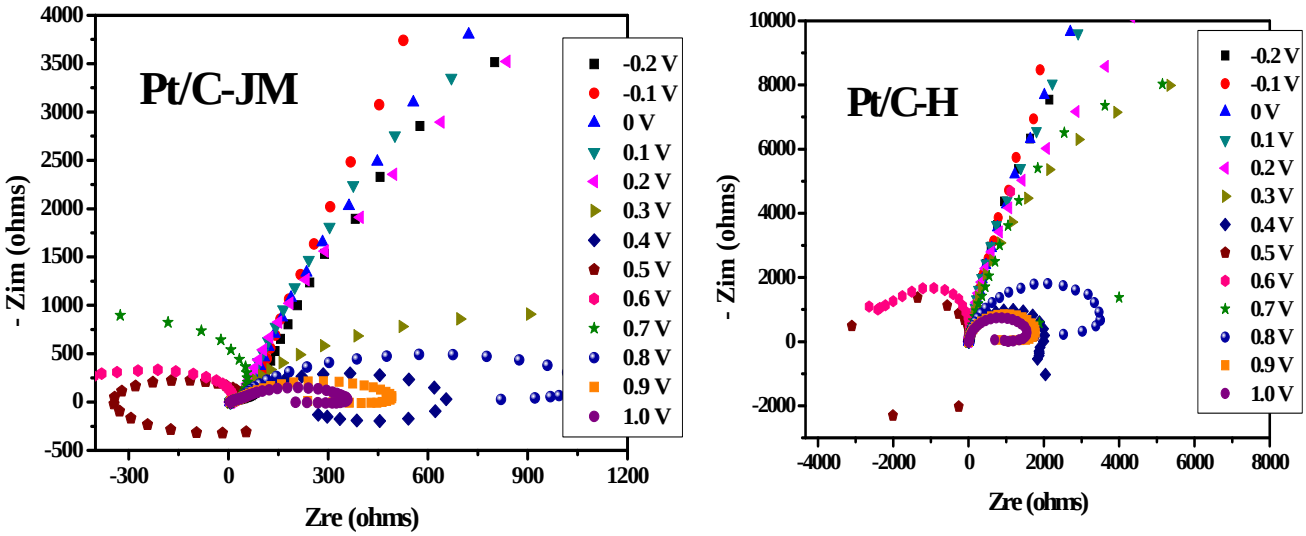

Figure S10. Nyquist plots (a)-(i) of the various catalysts in electrochemical methanol oxidation at different potentials in 0.5 H_2SO_4 solutions containing 1 M CH_3OH.

References

1. V. Radmilovic, H. A. Gasteiger and J. P.N. Ross, *J. Catal.*, 1994, **154**, 98-106.
2. G. Yang, Y. Li, R. K. Rana and J.-J. Zhu, *J. Mater. Chem. A*, 2013, **1**, 1754.
3. B. Xiong, Y. Zhou, Y. Zhao, J. Wang, X. Chen, R. O'Hayre and Z. Shao, *Carbon*, 2013, **52**, 181-192.
4. X. Zhao, J. Zhu, L. Liang, J. Liao, C. Liu and W. Xing, *J. Mater. Chem.*, 2012, **22**, 19718–19725.
5. H. Wu, H. Li, Y. Zhai, X. Xu and Y. Jin, *Adv Mater*, 2012, **24**, 1594-1597.
6. R. Wang, Y. Xie, K. Shi, J. Wang, C. Tian, P. Shen and H. Fu, *Chem. Eur. J.*, 2012, **18**, 7443-7451.
7. Y. Kang, J. B. Pyo, X. Ye, T. R. Gordon and C. B. Murray, *ACS NANO*, 2012, **6**, 5642-5647.
8. L. X. Ding, A. L. Wang, G. R. Li, Z. Q. Liu, W. X. Zhao, C. Y. Su and Y. X. Tong, *J. Am. Chem. Soc.*, 2012, **134**, 5730-5733.
9. L. X. Ding, G. R. Li, Z. L. Wang, Z. Q. Liu, H. Liu and Y. X. Tong, *Chem. Eur. J.*, 2012, **18**, 8386-8391.
10. M. Yin, Y. Huang, L. Liang, J. Liao, C. Liu and W. Xing, *Chem Commun (Camb)*, 2011, **47**, 8172-8174.
11. Y. Y. Chu, Z. B. Wang, Z. Z. Jiang, D. M. Gu and G. P. Yin, *Adv Mater*, 2011, **23**, 3100-3104.
12. Y. Paik, S. S. Kim and O. H. Han, *Angew. Chem. Int. Ed.*, 2008, **47**, 94-96.
13. A. Murthy, E. Lee and A. Manthiram, *Appl. catal. B: Environ.*, 2012, **121-122**, 154-161.
14. K. G. NISHANTH, P. SRIDHAR, S. PITCHUMANI and A. K. SHUKLA, *Bull. Mater. Sci.*, 2013, **36**, 353-359.
15. H. Du, B. Li, F. Kang, R. Fu and Y. Zeng, *Carbon*, 2007, **45**, 429-435.
16. J. Qi, L. Jiang, Q. Tang, S. Zhu, S. Wang, B. Yi and G. Sun, *Carbon*, 2012, **50**, 2824-2831.
17. V. T. Thanh Ho, K. C. Pillai, H.-L. Chou, C.-J. Pan, J. Rick, W.-N. Su, B.-J. Hwang, J.-F. Lee, H.-S. Sheu and W.-T. Chuang, *Energy Environ. Sci.*, 2011, **4**, 4194.
18. K.-S. Yao, Y.-C. Chen, C.-H. Chao, W.-F. Wang, S.-Y. Lien, H. C. Shih, T.-L. Chen and K.-W. Weng, *Thin Solid Films*, 2010, **518**, 7225-7228.
19. Q. Lv, M. Yin, X. Zhao, C. Li, C. Liu and W. Xing, *J. Power Sources*, 2012, **218**, 93-99.